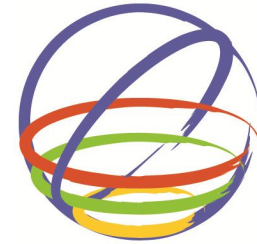


Experimental Study of Nonlinear Flexural and Shear Deformations of Reinforced Concrete Structural Walls

T. A. Tran & J. W. Wallace

University of California, Los Angeles



15 WCEE
LISBOA 2012

SUMMARY

An experimental study was conducted to provide insight into the nonlinear cyclic response of moderate-aspect ratio cantilever structural walls. Constant axial load and reversed cyclic loading were applied to five large-scale structural walls. Primary test variables were wall aspect ratio, wall axial stress, and wall shear stress. The test results indicate that significant lateral strength loss occurred at approximately 3.0% for all tests; however, various failure modes were observed. The contribution of nonlinear shear deformations to wall top lateral displacement varied between roughly 15% and 50%, for walls with aspect ratios of 2.0 and 1.5, respectively.

Keywords: nonlinear; flexural deformation; shear deformation; reinforced concrete; structural wall

1. INTRODUCTION

Reinforced concrete structural walls are very effective in resisting lateral loads due to their high strength and stiffness. ACI 318 code provisions for special structural walls were introduced in the 1970's and provisions for design of flexure-controlled walls were updated in ACI 318-99 based on a fairly robust body of analytical and experimental research. For moderate-aspect ratio walls, i.e., walls with aspect ratios between about 1.5 and 2.5, nonlinear shear behavior may be significant, leading to lower strength and stiffness, and larger concrete compressive strains; however, these factors are not typically considered in analysis and design.

Although a relatively significant number of tests have been conducted on moderate-rise walls (see Wood, 1990; Pilakoutas and Elnashai, 1995; Mickelborough et al., 1999; Salonikios et al., 1999, 2000), the tests tend to focus on the determination of wall shear strength, typically without axial load, and in many cases, provided web reinforcement or boundary transverse reinforcement do not satisfy ACI 318-99 (and later) requirements for special structural walls. In addition, and significantly, deformations associated with the test setup were not always measured and detailed instrumentation was rarely provided; therefore, the measured results may not be reliable for assessing deformation responses associated with different damage states (e.g., cracking, yielding, spalling, buckling, strength loss, residual strength, loss of vertical load carrying capacity). The lack of sufficient and precise instrumentation inhibits the development of robust analysis and design tools to enable development and use of more elegant and cost-effective approaches, such as Performance-Based Seismic Design.

A research program, with both analytical and experimental components, was undertaken to fill some of the identified knowledge gaps. The experimental phase of the research program is described. The test program included five large-scale reinforced concrete shear wall specimens designed such that nonlinear shear deformations were expected to contribute significantly to lateral displacement response. The test specimens were heavily instrumented to obtain detailed response information, as well as to provide data for development and validation of analytical models, including models that account for nonlinear shear-flexure interaction.

2. EXPERIMENTAL PROGRAM

2.1 Description of Test Specimens

Five large-scale reinforced concrete structural wall specimens, subjected to combined constant axial load and reversed cyclic lateral loading, were tested (Table 1). Specimen identifiers are used for quick reference, i.e., specimen **RW-A20-P10-S38**, describes a **R**ectangular **W**all with **A**spect ratio of **2.0** under design axial load **P** of **10%** $A_g f'_c$, and design average Shear stress of **3.8** $\sqrt{f'_c}$ psi ($0.32\sqrt{f'_c}$ MPa).

Primary test variables included aspect ratio (1.5 and 2.0), which was also shear-span ratio in this case, axial load level ($0.025A_g f'_c$ and $0.10A_g f'_c$), and wall shear stress level.

The five wall specimens are 6 in. (150 mm) thick and 48 in. (1220 mm) long, with lateral load applied at either 72 in. (1830 mm) or 96 in. (2440 mm) above the wall-foundation interface. Axial load levels of $0.10A_g f'_c$ and $0.025A_g f'_c$ were applied to the first four specimens and the fifth specimen, respectively, where f'_c is the design concrete compressive strength. The ratios of horizontal and vertical web reinforcement of each wall, ρ_t and ρ_l , respectively, were equal and exceeded the 0.0025 minimum required by ACI 318-11. The ratio of the area of vertical boundary reinforcement to the area of the boundary element ρ_b varied between 3.23% and 7.11%. Transverse reinforcement at wall boundaries satisfies ACI 318-11 S21.9.6.4 requirements for special structural walls.

Table 1. Wall Specimen Attributes

Test No.	Specimen code	h_w/l_w	$\rho_t = \rho_l$ (%)	ρ_b (%)	$V@M_n^{des}/V_n^{des}$	$P/A_g f'_c$	$V@M_n/V_n$	$V@M_n/A_{cv} \sqrt{f'_c}$
1	RW-A20-P10-S38	2.0	0.27	3.23	0.80	0.073	0.81	3.6
2	RW-A20-P10-S63		0.61	7.11	0.88	0.073	0.91	6.1
3	RW-A15-P10-S51	1.5	0.32	3.23	0.80	0.077	0.83	4.9
4	RW-A15-P10-S78		0.73	6.06	0.84	0.064	0.85	7.0
5	RW-A15-P2.5-S64		0.61	6.06	0.79	0.016	0.79	5.8

Notes: h_w/l_w is the aspect ratio; ρ_t is the horizontal web reinforcement ratio; ρ_l is the vertical web reinforcement ratio; ρ_b is the boundary longitudinal reinforcement ratio; $V@M_n^{des}/V_n^{des}$ is the design ratio of the lateral load corresponding to the nominal moment capacity over the nominal shear strength using the specified compressive strength of concrete and specified yield strength of reinforcement; $P/A_g f'_c$ is the actual axial load ratio using the actual axial load and actual compressive strength of concrete; $V@M_n/V_n$ is the actual ratio of the lateral load corresponding to the nominal moment capacity over the nominal shear strength using the actual material strengths; $V@M_n/A_{cv} \sqrt{f'_c}$ is the actual ratio of the average shear stress at nominal moment capacity over $\sqrt{f'_c}$ using the actual material strengths, for f'_c in psi units.

The walls were designed to yield in flexure prior to strength loss, with the level of shear stress at flexural yield as a primary variable. The ratio of the lateral load corresponding to nominal moment capacity over the nominal shear strength determined from using ACI 318-11 S21.9.4, $V@M_n/V_n$, varied from 0.79 to 0.88 for design material strengths, or very close to the design limit (for $\phi = 1.0$). A primary objective of the test program was to assess the impact of wall aspect ratio, the level of average shear stress and axial stress on the wall deformation capacity at significant loss of lateral load capacity, as well as the influence of these parameters on loss of axial load capacity.

2.2 Material Properties

Concrete clear cover over boundary vertical reinforcement was selected to be greater than or equal to one vertical boundary bar diameter (either US #4, #5, or #6); therefore, a maximum aggregate size of 3/8 in. (9.5 mm) was specified. For each wall specimen, three concrete cylinders were tested to obtain the average compressive strength. The average concrete compressive strength at test date for the first three specimens and the other two specimens were approximately 48 MPa and 56 MPa, respectively.

The strain at peak stress for all five specimens was approximately 0.0023. More details on material properties are provided by Tran and Wallace (2012).

Cross-section and reinforcement details of all five specimens are given in Fig. 1 and Table 2. Deformed reinforcement consisted of eight boundary vertical bars (either #4, #5, or #6), whereas web reinforcement consisted of two curtains of either #2 or #3 bars. Transverse reinforcement at the wall boundaries satisfied ACI 318-11 S21.9.6.4 requirements for special structural walls. Diameters of #2, #3, #4, #5, #6 are 1/4 in. (6.4 mm), 3/8 in. (9.5 mm), 1/2 in. (12.7 mm), 5/8 in. (15.9 mm), 3/4 in. (19.1 mm), respectively, whereas nominal diameters of the D6a and D6b reinforcement are 6 mm. Yield strength is approximately 475 MPa for #4, #5, #6 bars, 440 MPa for #2, #3, D6a bars, and 515 MPa for D6b bars. Ultimate strength of #2 is 490 MPa, while the average ultimate strength for all remaining reinforcement is approximately 635 MPa.

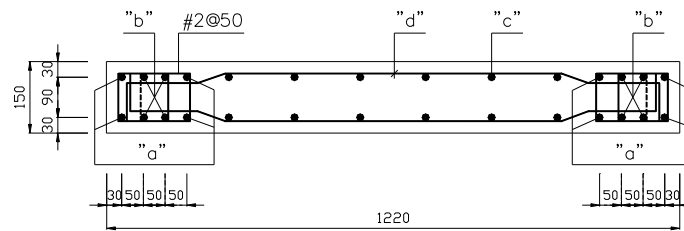


Figure 1. Wall reinforcement details

Table 2. Wall Reinforcement Details

Wall specimen	"a"	"b"	"c"	"d"
RW-A20-P10-S38	4#4	4#4	6D6a @140 (@5.5in.)	D6b @140 (@5.5in.)
RW-A20-P10-S63	4#6	4#6	5#3 @152 (@6in.)	#3 @152 (@6in.)
RW-A15-P10-S51	4#4	4#4	7D6a @114 (@4.5in.)	D6b @114 (@4.5in.)
RW-A15-P10-S78	4#6	4#5	6#3 @127 (@5in.)	#3 @127 (@5in.)
RW-A15-P2.5-S64	4#6	4#5	5#3 @152 (@6in.)	#3 @152 (@6in.)

2.3 Test Procedure

The cantilever wall specimens were tested in an upright position, with a horizontal lateral load applied 8 ft (2440 mm) and 6 ft (1830 mm) from the base of the wall for the aspect ratio 2.0 and 1.5 specimens, respectively. Axial load was applied using two, hollow cylinders connected to post-tensioning bars, one on each side of the wall (Fig. 2). The lateral load was applied through a friction mechanism using two plates, one on either wall face along with through-wall post-tensioning bars, to spread the lateral load uniformly across the top of the wall. The reversed cyclic lateral load was transmitted to the wall at a very slow rate. An out-of-plane support frame was used to prevent wall twisting.

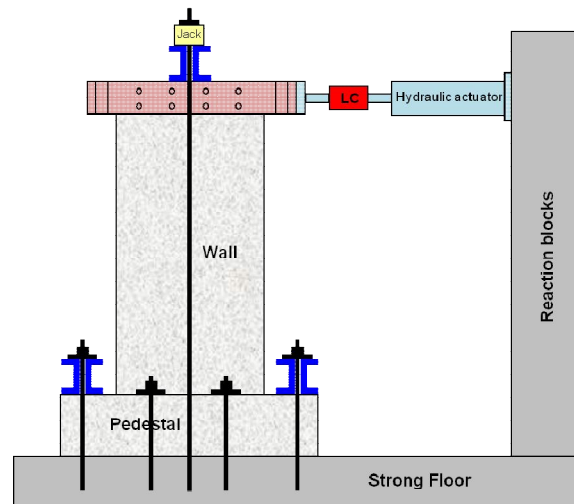


Figure 2. Schematic test setup

The testing protocol consisted of load-controlled, generally three cycles at $\frac{1}{4}$, $\frac{1}{2}$, and $\frac{3}{4}$ of the expected yield force, followed by displacement-controlled cycles, typically three cycles at top drift ratios of 0.375%, 0.5%, 0.75%, 1.0%, 1.5%, 2.0%, and two cycles at top drift ratios of 3.0%, and 4.0%.

2.4 Instrumentation

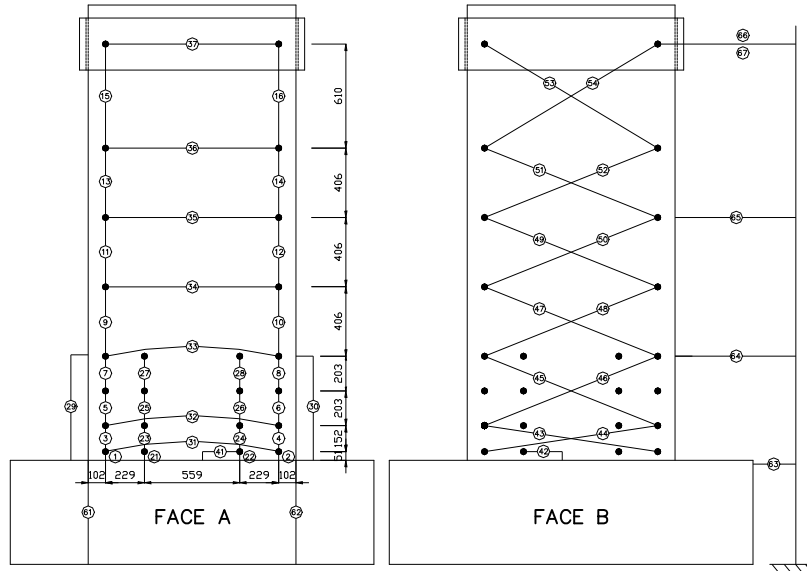


Figure 3 - Sensor configuration for specimens with aspect ratio 2.0

Load cells were used to measure the applied lateral and axial load. Linear variable differential transformers (LVDTs) were used to measure lateral wall displacements, wall foundation sliding and uplift, and to allow determination of wall average concrete strains over specified gauge lengths (e.g., to enable calculation of wall curvature). The LVDT layout for an aspect ratio 2.0 wall is shown in Fig. 3. Reinforcement strains were measured at 30 locations using strain

gauges affixed to vertical boundary reinforcement, vertical and horizontal web reinforcement, and transverse reinforcement over the height of about $l_w/2$ from the interface of the wall and the base.

3. TEST RESULTS AND DISCUSSIONS

Test results for all five specimens are summarized in Table 3, including lateral load and top displacement under both positive and negative loading at concrete cracking, boundary vertical reinforcement yielding, peak loading, and at significant loss of lateral strength. Observed damage, failure mode, and lateral load versus top displacement relations are presented and discussed in the following sections.

Table 3. Test Result Summary

Wall code	Loading direction	Cracking		Yielding		Peak load		Failure	
		F (kN)	Δ^{top} (mm)	F (kN)	Δ^{top} (mm)	F (kN)	Δ^{top} (mm)	F (kN)	Δ^{top} (mm)
RW-A20-P10-S38	Positive	148	2.0	379	13	481	56	445	76
	Negative	-143	-1.8	-374	-14	-436	-36	-413	-75
RW-A20-P10-S63	Positive	169	2.1	630	16	742	69	734	73
	Negative	-165	-2.0	-597	-15	-717	-69	-699	-73
RW-A15-P10-S51	Positive	190	1.3	527	10	603	52	485	60
	Negative	-189	-1.1	-506	-9	-575	-50	-567	-55
RW-A15-P10-S78	Positive	201	1.5	776	12	859	27	791	55
	Negative	-198	-1.1	-727	-11	-823	-27	-739	-55
RW-A15-P2.5-S64	Positive	142	1.3	627	11	670	27	543	55
	Negative	-141	-1.1	-588	-10	-660	-27	-364	-55

3.1 Specimen RW-A20-P10-S38

This wall had web reinforcement ratios of 0.0027, which is slightly greater than ACI 318-11 Section 21.9.2 minimum requirements for special structural walls of 0.0025. Data from strain gauges affixed to boundary longitudinal reinforcement indicated that the first yielding occurred when the top of the wall was displaced to +13 and -14 mm at lateral loads of +379 and -374 kN. At first yielding, the maximum crack widths were 0.15 mm for horizontal (flexural) cracks and 0.5 mm for diagonal (shear) cracks. At zero lateral load, residual crack widths for both horizontal and inclined cracks were 0.1 mm. Crack patterns at drift ratios of 0.5%, 1.5%, and at failure are shown in Fig. 4.

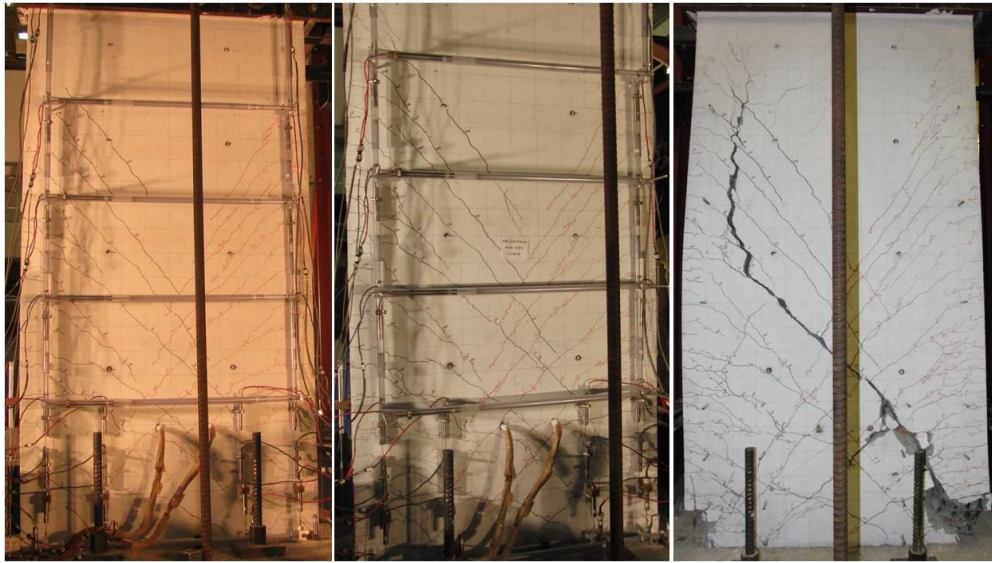


Figure 4. Crack patterns in specimen RW-A20-P10-S38 at drift ratios of 0.5%, 1.5%, and 3.0%

Slip and extension of longitudinal boundary reinforcement increased significantly at 0.75% drift, resulting in a crack running along the interface of the wall and the base. At a drift ratio of 1.0%, vertical cracks were observed at the wall boundary, followed by spalling of cover concrete at both wall ends adjacent to the wall-foundation interface. During the first cycle to 3.0% drift, cover concrete at wall boundaries from the wall-foundation interface to a height of about 175 mm had completely spalled off and flexural and shear cracks had maximum residual widths of 1.0 and 1.25 mm, respectively. During the second cycle to 3.0% drift, concrete in the core of the right (south) wall boundary crushed and boundary longitudinal reinforcement buckled under positive loading. Immediately following boundary bar buckling, a sudden diagonal tension failure occurred (Fig. 4), with fracture of horizontal web bars along the diagonal crack; lateral strength dropped from 415 to 147 kN, or to only 30% of the peak load. Lateral load versus top displacement is presented in Fig. 6a.

3.2 Specimen RW-A20-P10-S63

The second test specimen had the same aspect ratio and axial load ratio as the first test specimen, but a higher average shear stress ($6.1\sqrt{f'_c}$ versus $3.6\sqrt{f'_c}$ psi ; $0.51\sqrt{f'_c}$ versus $0.30\sqrt{f'_c}$ MPa). The higher shear demand was achieved by approximately doubling the boundary longitudinal steel; web reinforcement also approximately doubled due to the higher shear demands. Ideally, we might have preferred to test the same wall and changed the application of lateral load to achieve the test objective (change in moment-to-shear span ratio); however, this was not possible within the test budget.

First yielding of boundary longitudinal reinforcement occurred at lateral loads of +630 and -597 kN at wall top displacements of +16 and -15 mm. A horizontal crack at the wall-foundation interface and a few 100 mm-length vertical cracks at wall boundaries formed during cycles to 1.0% drift ratio. Wider

and longer vertical cracks were observed at these locations during subsequent cycles to higher drift levels. Spalling of cover concrete at each wall boundary was noted at 2.0% drift level (over approximately 70 mm from the wall-foundation interface) and extended up to about 110 mm during the first cycle of 3.0% drift. During the 3.0% lateral drift cycles, diagonal crack widths as large as 3.5 mm and horizontal (flexural) crack widths as large as 1.5 mm were measured; maximum residual cracks widths were 1.0 mm and 0.6 mm for diagonal and horizontal cracks, respectively.

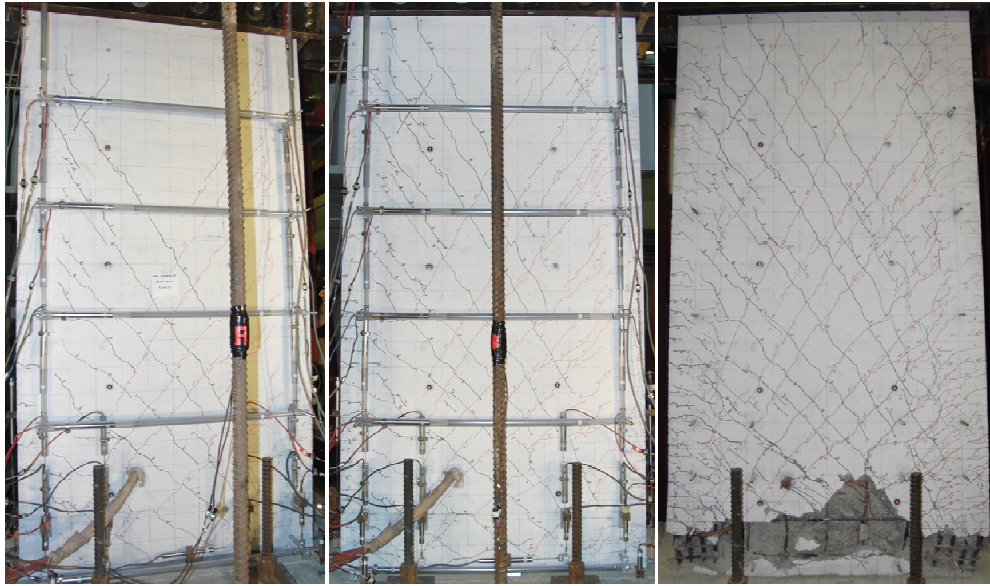


Figure 5. Crack patterns in specimen RW-A20-P10-S63 at drift ratios of 0.5%, 1.5%, and 3.0%

Lateral load capacity dropped to 39% of the peak load during the second cycle to 3.0% drift, due to crushing of concrete and buckling of vertical boundary and some vertical web reinforcement at the north wall boundary. When the loading was reversed, a similar failure mode was observed at the south wall boundary. Due to safety concerns, the test was stopped at drift ratio of 2.4% and a lateral force equal to 21% of the peak strength left. Fig. 5 presents cracking patterns at drift levels of 0.5%, 1.5%, and 3.0%. The horizontal load versus horizontal wall top displacement relation is presented in Fig. 6a.

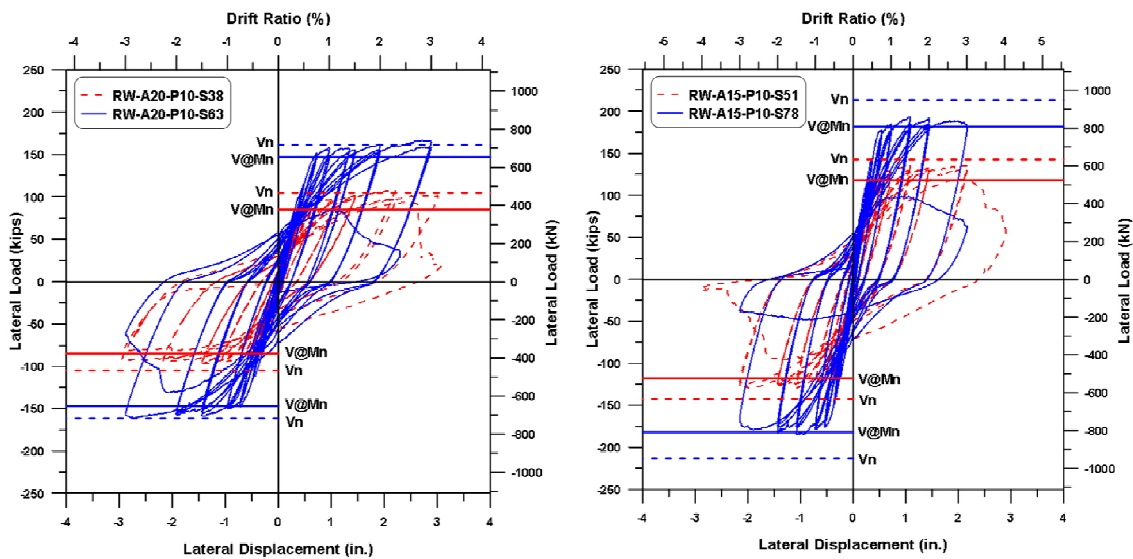


Figure 6. Lateral load versus top displacement for wall specimens

The relations presented in Fig. 6a for the aspect ratio 2.0 walls are very similar, even with the variation in shear demand, although the failure modes were quite different.

3.3 Specimen RW-A15-P10-S51

The third wall specimen had the same longitudinal boundary reinforcement and axial load ratios as the first wall specimen, but a lower aspect ratio (1.5 versus 2.0), and a slightly higher web reinforcement ratio (0.0032 versus 0.0027). Thus the lateral load corresponding to the nominal moment capacity was larger, leading to a higher design shear stress.

At a drift ratio of 1.0%, crack widths for horizontal and inclined cracks did not exceed 1.25 and 1.0 mm, respectively; the peak residual crack widths were 0.2 mm for flexural cracks and 0.1 mm for shear cracks. A few vertical cracks were observed at wall-foundation interface at wall boundaries at 0.75% drift, but extensive spalling of concrete cover was not observed until 1.5% drift. Peak lateral loads of +603 and -575 kN were reached during the first cycle to 3.0% drift. Signs of deterioration of core concrete at the wall boundaries were noted in the subsequent cycle. Crack widths at 3.0% drift reached 2.0 mm for horizontal cracks and 3.0 mm for diagonal cracks, whereas the maximum residual widths for both types of cracks were 0.8 mm. Crack patterns at drift ratios of 0.5%, 1.5%, and at failure are shown in Fig. 7.



Figure 7. Crack patterns in specimen RW-A15-P10-S51 at drift ratios of 0.5%, 1.5%, and at failure

When the wall was loaded in positive direction to 4.0% drift, crushing of core concrete of the south wall boundary and buckling of vertical boundary reinforcement occurred, which initiated diagonal tension failure along a major crack with an angle of about 40 degrees with the horizontal at the wall base (crack * in Fig. 7), with fracture of several horizontal web bars crossing the diagonal crack. As a result, the wall was able to resist only 41% of the peak strength at 4.0% drift. When reserved loading was applied, fracture of two longitudinal bars at the south wall boundary was observed, along with concrete crushing and buckling of longitudinal reinforcement at the north wall boundary, and the lateral load dropped to only 10% of the peak load (Fig. 6b).

3.4 Specimen RW-A15-P10-S78

This wall had the same aspect ratio and axial load level as wall RW-A15-P10-S51; however, the actual average shear stress for this specimen is much higher ($7.0\sqrt{f'_c}$ versus $4.9\sqrt{f'_c}$ psi or $0.58\sqrt{f'_c}$ versus $0.41\sqrt{f'_c}$ MPa). The horizontal load versus horizontal wall top displacement relation is presented in Fig. 6b, together with that of wall RW-A15-P10-S51.

First yielding of vertical boundary reinforcement was observed at drift ratios of +0.67% and -0.58%, which were slightly larger than those from wall RW-A15-P10-S51. At 1.0% drift, a crack crossing the wall-foundation interface appeared and two approximately 100 mm-length vertical cracks formed at the south wall boundary. Cover concrete spalling was observed over a length of 25 mm at 1.5% drift and it became more severe from 2.0% drift, with complete spalling of concrete at wall boundaries from the wall-foundation interface to a height of about 75 mm. Peak lateral load of +859 and -823 kN were measured at 1.5% lateral drift for positive and negative loading.

During the first cycle to 3.0% drift, modest spalling of cover concrete was observed along diagonal compressive concrete struts near the wall-foundation interface at the wall boundaries. Accordingly, the lateral strength of the wall decreased to 92% and 90% of the peak load in positive and negative directions, respectively. At this drift level, maximum crack widths were 2.0 and 3.0 mm, and maximum residual crack widths were 1.0 and 1.25 mm, for horizontal and inclined cracks, respectively. As the wall was loaded in the positive direction during the second cycle to 3.0% drift, shear sliding was observed, followed by out-of-plane buckling at the south wall boundary. As a result, the wall lost about two-thirds of its peak lateral strength. When loading was reversed, out-of-plane buckling occurred at the north wall boundary, and the lateral load capacity dropped to only 20% of the peak lateral load. Crack patterns at drift ratios of 0.5%, 1.5%, and 3.0% are shown in Fig. 8.

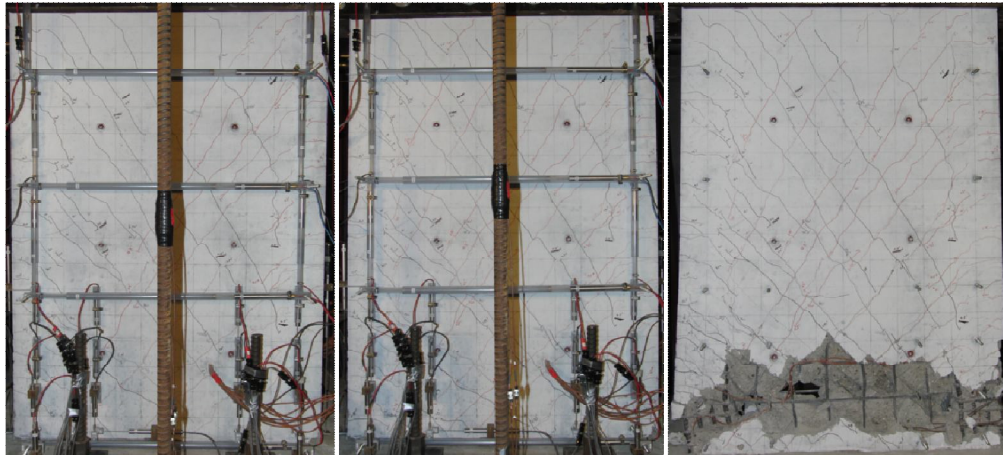


Figure 8. Crack patterns in specimen RW-A15-P10-S78 at drift ratios of 0.5%, 1.5%, and 3.0%

3.5 Specimen RW-A15-P2.5-S64

This test specimen had the same reinforcement configuration as specimen RW-A15-P10-S78, except a slightly smaller web reinforcement ratio. The main difference between these two walls was the axial load ratio, i.e., the axial load ratio of wall RW-A15-P2.5-S64 was only one-fourth of that of RW-A15-P10-S78 (0.016 versus 0.064).

First yielding of boundary longitudinal reinforcement was observed at drift ratios of +0.61% and -0.56%, which were slightly less than those from RW-A15-P10-S78. Slip and extension of vertical reinforcement became significant at 0.75% drift, leading to the appearance of a horizontal crack at the wall-foundation interface. Vertical cracks were observed at the foundation-wall interface at wall boundaries at 1.0% drift, indicating initial concrete cover spalling; spalling of cover concrete occurred over a length of 75 mm at the wall base at 2.0% drift. Maximum inclined crack widths in walls RW-A15-P2.5-S64 and RW-A15-P10-S78 were 2.0 and 1.5 mm at 1.5% drift, and were 3.0 and 2.0 mm at 2.0% drift, respectively.

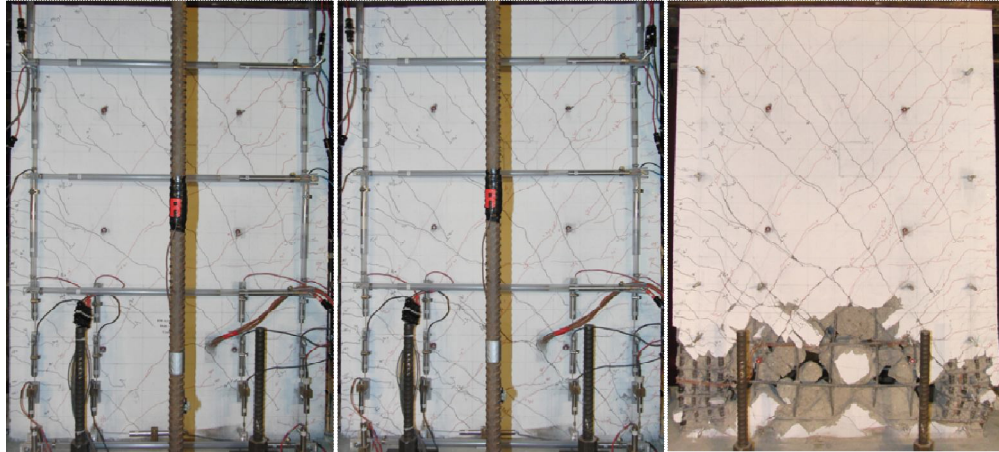


Figure 9. Crack patterns in specimen RW-A15-P2.5-S64 at drift ratios of 0.5%, 1.5%, and 3.0%

Crack patterns at various drift ratios are presented in Fig. 9 and the lateral load versus top lateral displacement relation is presented in Fig. 10. The wall reached its maximum lateral capacity at a drift ratio of 1.5%, which was identical to wall RW-A15-P10-S78; however, its peak strength was only about 80% of that of RW-A15-P10-S78. Similar to wall RW-A15-P10-S78, during the first cycle to 3.0% drift, modest spalling of cover concrete was observed along diagonal compressive concrete struts near the wall-foundation interface at the wall boundaries. As a result, the wall lateral load decreased to 81% and 55% of the peak load in positive and negative directions, respectively. Shear sliding was observed during the subsequent cycle, causing a substantial reduction of the wall lateral load to only 36% and 26% of the peak strength in two directions. Vertical boundary reinforcement buckled in the direction of the applied load (in-plane, Fig. 9), versus the out-of-plane instability that was observed in RW-A15-P10-S78 with higher axial load.

3.6 Flexural and Shear Deformations

Diagrams of lateral load versus shear and total displacements for specimens RW-A15-P10-S78 and RW-A15-P2.5-S64 are presented in Fig. 10. The figure shows that nonlinear shear deformations

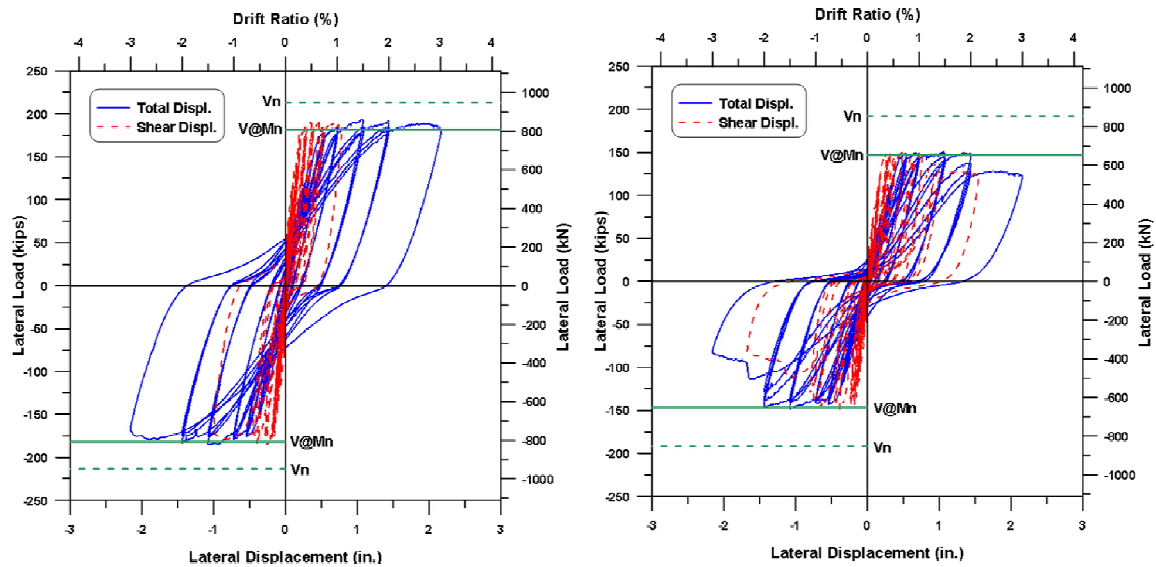


Figure 10. Lateral load versus shear and total displacements
(a) Specimen RW-A15-P10-S78; (b) Specimen RW-A15-P2.5-S64

accounted for approximately 35 and 50 percent of the top lateral displacement in walls RW-A15-P10-S78 and RW-A15-P2.5-S64, respectively. In addition, inelastic flexural and shear deformations initiated simultaneously at the same lateral load level, even though these loads were only about 80 and 75 percent of the nominal wall shear strength. The observed interaction between flexural and shear responses is consistent with previous findings (e.g., Massone and Wallace, 2004). The contribution of shear deformations to wall top displacement in the aspect ratio 2.0 walls was lower than that for the aspect ratio 1.5 walls, ranging from about 15 percent in specimen RW-A20-P10-S38 to nearly 30 percent in specimen RW-A20-P10-S63.

4. CONCLUSIONS

Test results for moderate-aspect ratio cantilever walls indicate significant lateral strength loss at approximately 3.0% for all tests; however, significant lateral strength loss was observed for a variety of reasons, i.e., diagonal tension, web crushing, sliding shear, and buckling of vertical reinforcement. The results indicate that strength loss (failure) is impacted by aspect ratio, average shear stress level, axial load level, and vertical and horizontal reinforcement ratios. The contribution of nonlinear shear deformations to wall top lateral displacement varied between approximately 15% and 50%, with lower values for the aspect ratio 2.0 walls. The detailed data collected in the tests will be used to validate models for cyclic shear-flexure interaction.

ACKNOWLEDGEMENTS

The work presented in this paper was supported by fund from the National Science Foundation under Grant NSF CMMI-0825347. This research was performed in a collaboratory renovated with funds provided by the National Science Foundation under Grant No. 0963183, which is an award funded under the American Recovery and Reinvestment Act of 2009 (ARRA). The assistance of Dr. A. Salamanca and Senior Development Engineer S. Keowen, as well as UCLA graduate student C. Hilson, are greatly appreciated. Undergraduate laboratory assistants B. Gerlick, R. Marapao, G. Schwartz, NEES and CENS summer interns K. Weiland, S. Garcia, I. Wallace, L. Herrera, J. Diaz, and F. Cifelli also helped complete the testing program. Any opinions, findings, and conclusions expressed in this paper are those of the authors and do not necessarily reflect those of the supporting organization or other people acknowledged herein.

REFERENCES

- [1] ACI Committee 318 (1999). Building Code Requirements for Structural Concrete (ACI 318-99) and Commentary. American Concrete Institute, Farmington Hills, Michigan, 391 pp.
- [2] ACI Committee 318 (2011). Building Code Requirements for Structural Concrete (ACI 318-11) and Commentary. American Concrete Institute, Farmington Hills, Michigan, 503 pp.
- [3] Massone and Wallace (2004). Load-Deformation Responses of Slender Reinforced Concrete Walls. *ACI Structural Journal*. **V. 101: No. 1**, 103-113.
- [4] Mickleborough et al. (1999). Prediction of Stiffness of Reinforced Concrete Shearwalls under Service Loads. *ACI Structural Journal*. **V. 96: No. 6**, 1018-1026.
- [5] Pilakoutas and Elnashai (1995). Cyclic Behavior of Reinforced Concrete Cantilever Walls, Part I: Experimental Results. *ACI Structural Journal*. **V. 92: No. 3**, 271-281.
- [6] Pilakoutas and Elnashai (1995). Cyclic Behavior of Reinforced Concrete Cantilever Walls, Part II: Discussions and Theoretical Comparisons. *ACI Structural Journal*. **V. 92: No. 4**, 425-433.
- [7] Salonikios et al. (1999). Cyclic Load Behavior of Low-Slenderness Reinforced Concrete Walls: Design Basis and Test Results. *ACI Structural Journal*. **V. 96: No. 4**, 649-660.
- [8] Salonikios et al. (2000). Cyclic Load Behavior of Low-Slenderness Reinforced Concrete Walls: Failure Modes, Strength and Deformation Analysis, and Design Implications. *ACI Structural Journal*. **V. 97: No. 1**, 132-142.
- [9] Tran, T.A. and Wallace, J.W. (2012). Experimental Study of the Lateral Load Response of Moderate Aspect Ratio Reinforced Concrete Structural Walls. Report No. UCLA SGEL 2012/XX, Department of Civil Engineering, University of California, Los Angeles, zz pp.
- [10] Wood, S.L. (1990). Shear Strength of Low-Rise Reinforced Concrete Walls. *ACI Structural Journal*. **V87: No. 1**, 99-107.